



**HAL**  
open science

## Vesicle tumbling inhibited by inertia

Aymen Laadhari, Pierre Saramito, Chaouqi Misbah

► **To cite this version:**

Aymen Laadhari, Pierre Saramito, Chaouqi Misbah. Vesicle tumbling inhibited by inertia. 2011. hal-00604401v1

**HAL Id: hal-00604401**

**<https://hal.science/hal-00604401v1>**

Preprint submitted on 28 Jun 2011 (v1), last revised 1 Jul 2011 (v2)

**HAL** is a multi-disciplinary open access archive for the deposit and dissemination of scientific research documents, whether they are published or not. The documents may come from teaching and research institutions in France or abroad, or from public or private research centers.

L'archive ouverte pluridisciplinaire **HAL**, est destinée au dépôt et à la diffusion de documents scientifiques de niveau recherche, publiés ou non, émanant des établissements d'enseignement et de recherche français ou étrangers, des laboratoires publics ou privés.

# Vesicle tumbling inhibited by inertia

Aymen Laadhari,<sup>1</sup> Pierre Saramito,<sup>1</sup> and Chaouqi Misbah<sup>2</sup>

<sup>1)</sup> *Université de Grenoble 1/CNRS, Laboratoire Jean Kuntzmann, B. P. 53, 38041 Grenoble Cedex 9, France*

<sup>2)</sup> *Université de Grenoble 1/CNRS, Laboratoire Interdisciplinaire de Physique/ UMR5588 F-38041, France*

Vesicles under flow constitute a model system for studying red blood cells (RBCs) dynamics and blood rheology. In the blood circulatory system the Reynolds number (at the scale of the RBC) may attain few unities. We develop a numerical method based on the the level set approach and solve the fluid/membrane coupling by using an adaptative finite element technique. We find that inertia can destroy completely the vesicle tumbling motion obtained in the Stokes regime. We analyze in details this phenomenon and discuss some of the far reaching consequences.

PACS numbers: 87.16.D- 83.50.Ha 87.17.Jj 83.80.Lz 87.19.rh

## I. INTRODUCTION

The study of models of red blood cells (RBCs), such as capsules and vesicles, has known recently a considerable amount of interest in various communities, such as physics, applied mathematics, mechanical engineering, and so on. A systematic experimental analysis<sup>1</sup> of RBCs under shear flow has revealed that RBCs can either undergo a tank-treading (TT) or tumbling (TB) motion. In the TT regime the main axis makes a given angle (less than  $\pi/4$ ) with respect to the flow direction whereas the RBCs membrane undergoes a tank-treading motion. Upon increasing the viscosity contrast  $\lambda$  (ratio of the internal over the external fluid viscosities) the RBC exhibits TB (or flipping) motion. There are two classes of model systems that are used to mimic RBCs : (i) capsules and (ii) vesicles. Capsules are made of an *extensible* polymer membrane which is endowed with an in-plane shear elasticity (mimicking the elasticity of the cytoskeleton of the RBCs)<sup>2</sup>. Vesicles are, like RBCs, made of an *inextensible* phospholipid bilayer membrane which is purely fluid (thus devoid of shear elasticity). The inextensible character has proven to confer to vesicles rich dynamics<sup>3,4</sup>, since inextensibility, triggers, even to leading order, high order nonlinearities.

An early model to understand the TT-TB transition of RBCs has been studied by Keller and Skalak (KS)<sup>5</sup>. They adopted a vesicle-like model (fluid inextensible membrane), and imposed a fixed shape (only orientation in the flow is permitted). The shape of the vesicle is assumed to be ellipsoidal for which a solution for the Stokes flow was available. KS reported that the transition depends both on the viscosity contrast  $\lambda$  and on the reduced volume  $v$  (the actual volume over the volume of a sphere having the same area). Numerical simulations in two dimensions<sup>6,7</sup> allowing for the shape to freely deform deformable shapes have revealed that the KS model constitute a very good approximation.

The analytical as well as numerical calculations<sup>6,7</sup> for the TT-TB transition<sup>5,8</sup> have been restricted to the

Stokes limit (inertia was neglected). Most of experimental data on vesicles<sup>9,10</sup> were available in the limit of small Reynolds numbers. In the blood circulatory system, except in capillaries, the Reynolds number evaluated at the scale of the RBC can reach few unities. For example, in the arterioles<sup>11</sup> the mean velocities is of about  $U \sim 20\text{cm/s}$ . Defining the Reynolds number as  $Re = \rho_o DU/\eta_o$  where  $D$  is the RBC diameter (is the diameter of a sphere having the same area as the RBC; it equal to about  $6\ \mu\text{m}$  for human RBCs),  $\eta_o$  the plasma viscosity and  $\rho_o$  its density. This leads to  $Re \sim 1$  in arterioles. This means that the inertial effect are, at least, of the same order as the viscous effects.

Our main objective in this study is to analyze the dynamics of vesicles under a shear flow by taking into account the inertial effects. Our study reveals that a Reynolds number of order unity is capable of inhibiting TB in favor of TT motion. We analyze the phase diagram in the relevant parameter space, and point out several implications and discuss more accurately the inertial effects and the experimental feasibility to test this prediction.

## II. MODEL AND TECHNIQUES

We consider a 2D vesicle under a linear shear flow. The legitimacy of a 2D geometry is supported by the fact that the 2D dynamics obtained in numerical simulations<sup>6,7</sup> reproduced the main results obtained in 3D by Keller and Skalak. Hereafter  $\mathbf{r}$  will denote a two dimensional position vector having the Cartesian components  $x$  (along the imposed flow) and  $y$  (the coordinate in the perpendicular direction). The vesicle is immersed in a fluid occupying a square domain of lateral length  $2L$ . Let  $R$  be the radius of a circle having the same perimeter as the vesicle. The aspect ratio is given by  $R/L$ . The scheme useful notations are presented in Fig. 1. The shear flow  $u_x = \pm V$  is prescribed at the top and bottom plates  $y = \pm L$  (see Fig. 1).

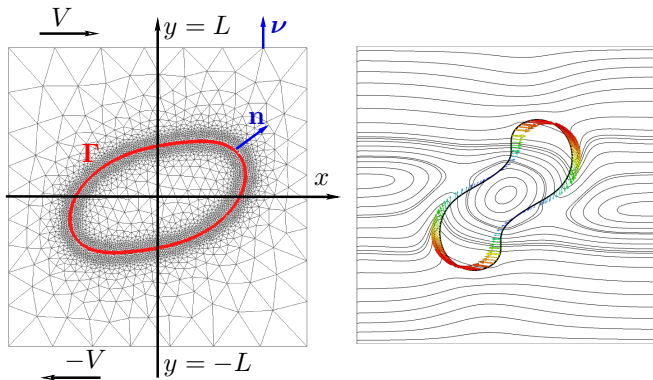


Figure 1. (color on-line) The set-up and notations. Actually the vesicle shapes shown here are obtained by numerical simulations. Left: a vesicle with a weak inertia ( $Re = 0.01$ ) in the TT regime. Right: a vesicle with inertia  $Re = 10$  showing ample vesicle deformation as compared to Stokes limit. Shown also the finite element network and the flow lines.

The velocity and pressure fields obey in the two fluid domains (inside and outside the vesicle)

$$\rho \left( \frac{\partial \mathbf{u}}{\partial t} + \mathbf{u} \cdot \nabla \mathbf{u} \right) - \mathbf{div} (2\eta D(\mathbf{u})) + \nabla p = 0$$

$$\mathbf{div} \mathbf{u} = 0$$

where  $D(\mathbf{u}) = (\nabla \mathbf{u} + \nabla \mathbf{u}^T)/2$  is the deformation rate tensor. At the vesicle membrane the hydrodynamic stress is balanced by the the membrane force

$$-\kappa \left\{ \frac{\partial^2 H}{\partial s^2} + \frac{H^3}{2} \right\} \mathbf{n}$$

$$+ H \zeta \mathbf{n} - \frac{\partial \zeta}{\partial s} \mathbf{t} + [2\eta D(\mathbf{u}) - pI] \cdot \mathbf{n} = 0$$

where  $\kappa$  is the membrane bending rigidity,  $H$  is the curvature,  $\mathbf{n}$  and  $\mathbf{t}$  are the normal and tangential unit vectors, and  $\zeta$  is a Lagrange multiplier enforcing locally constant arclength. It is fixed by requiring the surface divergence of the velocity field to vanish

$$\mathbf{div}_s \mathbf{u} = 0$$

In the upper and lower bounding boundaries we impose no-slip condition, while on the lateral size ( $y = \pm L$ ; see Fig. 1) we impose free surface where the total normal hydrodynamical force vanishes.

The above bulk equations (the Navier-Stokes equations) are nonlinear and the quite precise method based on boundary integral formulation<sup>7,12</sup> can not be used. The method we use here to solve the model equation is based on the level set approach. Very briefly, in this method the membrane location is defined by a level set function  $\phi(\mathbf{r}, t)$  depending on the 2D vector  $\mathbf{r} = (x, y)$  and time. The membrane position is taken to be (this is an implicit representation of the membrane)  $\phi = 0$ , which obeys a transport equation

$$\frac{\partial \phi}{\partial t} + \mathbf{u} \cdot \nabla \phi = 0$$

$\phi$  is defined everywhere in the entire domain, allowing to solve the fluid/structure problem in a fully Eulerian scheme. Indeed, the normal and the tangent vectors, as well as the curvature are defined in terms of  $\phi$ :  $\mathbf{n} = \nabla \phi / |\nabla \phi|$ ,  $H = \mathbf{div} \mathbf{n}$ , so that the full membrane force can be defined in the entire domain. The Lagrange multiplier is also defined in the entire domain. The full membrane force at the membrane is therefore defined in the entire domain, albeit its action is localized to the membrane region.

The above set of equations has been reformulated in terms of a variational representation (the so-called weak formulation) and has been implemented in a finite element scheme. Several numerical technical problems arise, such as vesicle bulk loss, membrane extension (or compression). In addition the level set function, which is initially a distance function, loses this property in the course of time, and has thus to be re-initialized to a distance function. Details of the numerical study and benchmark tests are published elsewhere<sup>13</sup>, and we focus here on the main physical results.

We have dimensionalized the equations by choosing  $R$  as a length scale,  $U = VR/L$  as a velocity scale,  $T = R/U$  as a unit of time and  $\eta_o U/R$  as a unit of pressure. This leads us to three dimensionless physical parameters

$$Re = \frac{\rho_o V R^2}{\eta_o}, \quad Ca = \frac{\eta_o R^3 \dot{\gamma}}{\kappa}, \quad \lambda = \frac{\eta_i}{\eta_o}$$

where  $\eta_i$  and  $\eta_o$  designate the internal and external viscosities. This set has to be supplemented with two geometrical parameters, namely the vesicle confinement  $Cn = R/L$  and the reduced area  $v = \mathcal{A}/(\pi(\mathcal{P}/2\pi)^2)$ , where  $\mathcal{A}$  is the area occupied by the internal liquid and  $\mathcal{P}$  is the vesicle perimeter.

Here we shall take the same densities, and we shall keep the confinement to a given value (typically 0.4). Moreover, in 2D, the TT-TB transition is quasi-insensitive to  $Ca$ <sup>7,14</sup>, so that we fix  $Ca = 100$  (and have checked that higher values do not affect the results). We are thus left with 3 free parameters  $v$ ,  $\lambda$  and  $Re$  (but we have also explored other values of  $Cn$  for comparison with previous results in the absence of inertia; see below).

### III. RESULTS AND DISCUSSION

We have first examined the low Reynolds number limit in order to test and validate our analysis by comparison to available numerical data in the Stokes regime. In that regime we are left with the parameters  $Ca$ ,  $v$  and  $\lambda$ . We have set  $Re = 10^{-2}$  which constitutes a good approximation to the Stokes regime. We have varied the two parameters  $\lambda$ ,  $v$  and have determined the transition line separating the regime of tank-treading (TT) from that of tumbling (TB). The results are shown in Fig. 2. The two results obtained are in a good agreement with the phase field methods<sup>7</sup> and also the 2D Keller and Skalak theory<sup>5</sup>. In our computations, a weak confinement  $Cn = 0.25$  has

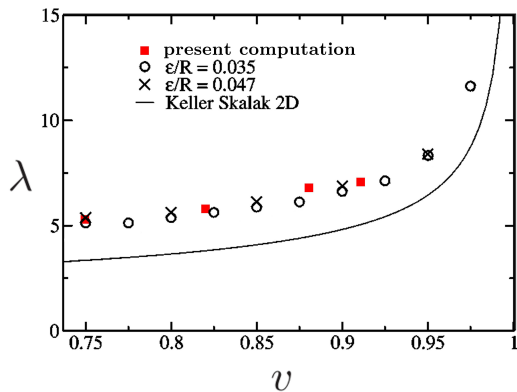


Figure 2. Phase diagram and comparison with other computations.

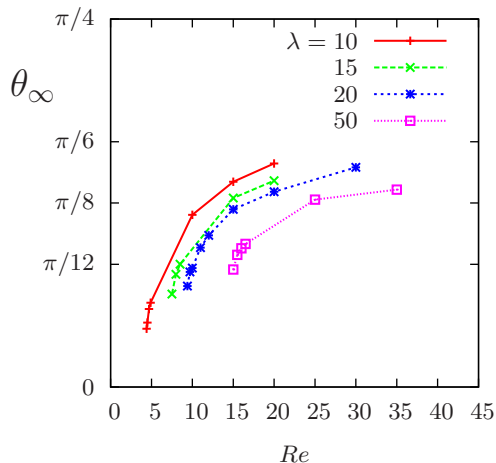


Figure 3. The behavior of the terminal angle  $\theta_\infty$  in the TT regime vs  $Re$  for various viscosity ratio  $\lambda$ .

been chosen, so that the influence of boundaries be weak enough (see also<sup>13</sup>).

Next we examine the role of the Reynolds number on the the two dynamical regime TT and TB. A first noticeable effect, is that upon increasing  $Re$  in the TB regime the period of oscillation increases significantly (Fig. 5) until it diverges (Fig. 4) for a critical value of  $Re$ . The interesting fact is that this behavior occurs for quite moderate values of  $Re$ . The divergence of the period means that the TB is suppressed in favor of a tank-treading regime. Another impact of the inertial effect is that the vesicle adopts in the TT regime a terminal angle that significantly depends on  $Re$ ; the terminal angle can have values which may be twice as large as compared to the corresponding values Stokes regime (see Fig. 3). Furthermore, the effect of inertia causes a stronger deformation of the vesicle, as shown on Fig. 1.

Our current intuitive understanding is as follows. In the absence of inertia TB occurs<sup>8</sup> when the viscosity contrast reaches a critical value such that the torque due to the applied shear flow can not anymore be efficiently con-

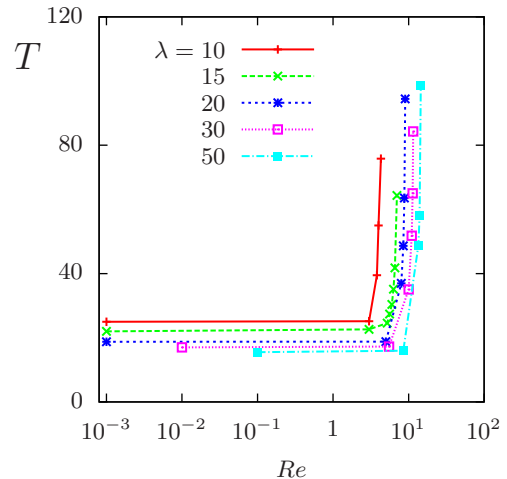


Figure 4. The behavior of the TB period  $T$  vs  $Re$  for various viscosity ratio  $\lambda$ , showing divergence of the period at a critical Reynolds number.

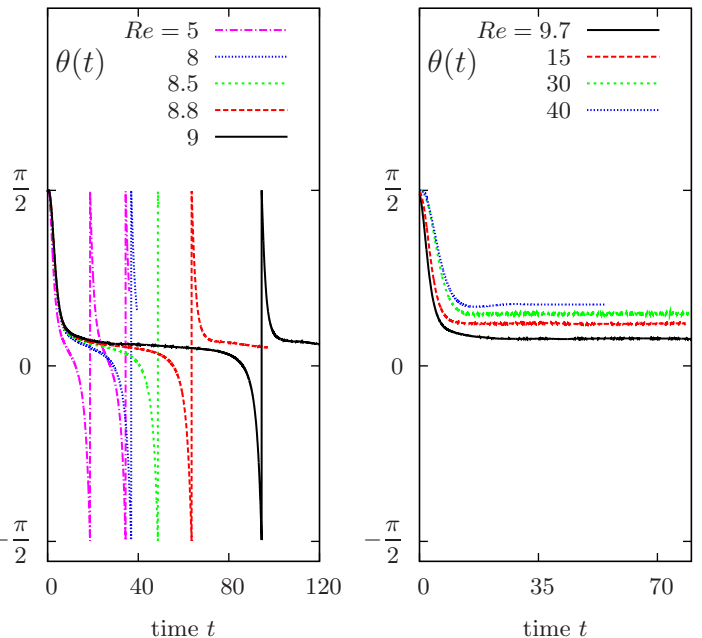


Figure 5. The behavior of the angle of the main axis of the vesicle as a function of time for different Reynolds numbers, showing that inertia slows down the motion, until suppressing TB .

verted into the membrane tank-treading torque because the internal fluid is so viscous that it precludes tank-treading. Therefore the vesicle behaves as almost quasi-rigid, and TB takes place. In other words, in the TB regime, the injected power due to shear is predominantly transferred to dissipation of the surrounding fluid. TB in the presence of inertia must, besides dissipation in the surrounding fluid, be accompanied with kinetic energy transfer to the surrounding fluid, a cost that increases with Reynolds number so that TB becomes unfavorable.

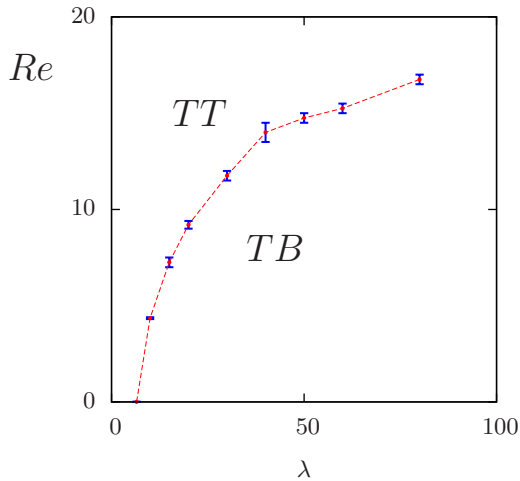


Figure 6. The phase diagram of the TT and TB motion as a function of the viscosity contrast  $\lambda$  and the Reynolds numbers. We have set  $v = 0.82$ ,  $Ca = 100$ ,  $Cn = 0.5$  and the critical Reynolds number is denoted by  $Re^*$ .

We have performed a systematic analysis (at fixed reduced area  $v = 0.82$ ) on the occurrence of TT and TB as a function of the viscosity contrast  $\lambda$  and Reynolds number  $Re$ . The results are reported on Fig. 6. In the absence of inertia ( $Re = 0$ ) the TT-TB bifurcation occurs at about  $\lambda = 6$ . As  $Re$  is increased TB is delayed. For example, at  $Re \simeq 5$  the critical  $\lambda$  has approximately doubled (it is about 12). It is interesting to note that the separation line in Fig. 6 attains a plateau at about  $Re = 20$  meaning that whatever the viscosity ratio is TB is completely suppressed (we have explored viscosity ratios of about 100). Actually, despite the fact that at  $\lambda \simeq 100$  the vesicle might be thought of as behaving as rigid-like particle (in which case one would expect TB to prevail) inertia is still capable of enforcing membrane tank-treading, making therefore the vesicle still to enjoy its fluidity.

Finally, let us make some general discussions. In the human arterioles the wall shear rate is of about  $8000 \text{ s}^{-1}$ , and using our definition of  $Re$ ,  $Re = \frac{\rho_o V R^2}{\eta_o}$ , with  $R \simeq 3 \mu\text{m}$ , and  $\eta_o/\rho_o \simeq 10^{-2} \text{ cm}^2/\text{s}$  (plasma kinematic viscosity), one obtains  $Re \sim 0.1$ . During entrance of cells in bifurcations of the circulatory network, cells undergo sudden changes of directions that momentarily enhance the shear gradient, resulting in higher  $Re$ . We are not aware of a systematic analysis of TB mimicking physiological conditions (especially the internal viscosity is temperature-dependent) in order to determine the precise value of the critical  $\lambda$ ,  $\lambda_c$ , at which transition from TT to TB occurs. Observation in arterioles show that isolated enough RBCs exhibit TB. This would mean that the actual viscosity ratio for RBCs,  $\lambda_{RBC}$  is larger than  $\lambda_c$ . Theoretical calculation on model systems (like vesicles and capsules) seem to support the idea that  $\lambda_{RBC}$  is

quite close to  $\lambda_c$ . This means that a small enough inertial effect may suppress TB.

Why should it be beneficial for RBCs to perform TT rather than TB a all? Cells which tend to approach a wall due, for example, to an alteration of the flow, resulting from a tissue injury (or due to an abnormal widening of blood vessels; the so-called sites of aneurysms), is expected to experience a lift force of hydrodynamical (viscous) nature<sup>10,15</sup>. This force is essential to keep cells away from potential undesirable adhesion. However, RBCs which undergo TB experience practically no lift force (due to the quasi-up-down symmetry over a period of TB)<sup>16</sup>. Due to an alteration of the flow (like bifurcations, aneurysm..) it is known that blood elements may tend to scrape along the blood vessel lining. The sudden change of the flow is expected to be accompanied with an increase of inertial effects that may suppress TB allowing for a lift force keeping RBCs away from the wall.

The present predictions are not devoid of experimental testability. Vesicles have large enough vesicle sizes (with radius in the range  $20 - 40 \mu\text{m}$ ). Imposing wall shear rates of about  $8000 \text{ s}^{-1}$  one finds  $Re \simeq 1 - 15$ . In a microfluidic channel of diameter  $d$ , with maximum velocity  $V_{max}$  of the imposed Poiseuille flow, the wall shear rate is equal to  $8V_{max}/d$ . Imposing a maximum velocity of order  $10 \text{ cm/s}$  (for which modern high speed camera can capture the vesicle motion with a good precision), one easily obtain shear rates of order  $10^4 \text{ s}^{-1}$ . We hope that this work will incite new experiments in order to identify the precise role of inertia.

C.M. and A.L. Acknowledge financial support from CNES and ANR (MOSICOB project).

## REFERENCES

- <sup>1</sup>T. Fischer, M. Stohr-Lissen, and H. Schmid-Schonbein, *Science* **202**, 894 (1978).
- <sup>2</sup>D. Barths-Biesel, C. R. *Physique* **10**, 764 (2009).
- <sup>3</sup>C. Misbah, *Phys. Rev. Lett.* **96**, 028104 (2006).
- <sup>4</sup>P. M. Vlahovska and R. S. Gracia, *Phys. Rev. E* **75**, 016313 (2007).
- <sup>5</sup>S. Keller and R. Skalak, *J. Fluid Mech.* **120**, 27 (1982).
- <sup>6</sup>T. Biben and C. Misbah, *Phys. Rev. E* **67**, 031908 (2003).
- <sup>7</sup>J. Beaucourt, F. Rioual, T. Seon, T. Biben, , and C. Misbah, *Phys. Rev. E* **69**, 011906 (2004).
- <sup>8</sup>F. Rioual, T. Biben, , and C. Misbah, *Phys. Rev. E* **69**, 061914 (2004).
- <sup>9</sup>V. Kantsler and V. Steinberg, *Phys. Rev. Lett.* **96**, 036001 (2006).
- <sup>10</sup>M.-A. Mader, V. Vitkova, M. Abkarian, A. Viallat, and T. Podgorski, *Eur. Phys. J. E* **19**, 389 (2006).
- <sup>11</sup>Y. C. Fung, Springer, New York(1990).
- <sup>12</sup>S. K. Veerapaneni, R. Raj, G. Biros, and P. K. Purohit, *International Journal of Non-Linear Mechanics* **44**, 257 (2009).
- <sup>13</sup>A. Laadhari, P. Saramito, and C. Misbah, *submitted*(2011), <http://hal.cnrs.fr/papiernum>.
- <sup>14</sup>G. Ghigliotti, T. Biben, and C. Misbah, *J. Fluid Mech.*(2010).
- <sup>15</sup>W. Wintz, H. Dobreiner, and U. Seifert, *Europhys. Lett.* **33**, 403 (1996).
- <sup>16</sup>G. Danker, T. Biben, T. Podgorski, C. Verdier, and C. Misbah, *Phys. Rev. E* **76**, 041905 (2007).